Transition Met Chem (2016) 41:213–223
DOI 10.1007/s11243-015-0013-4

Three 2D mixed-ligand Co(II) coordination polymers containing flexible bis(benzimidazole) ligands with different spacers

Xu Zhang[1] · Yong Guang Liu[1] · BaoYi Yu[2] · Guang Hua Cui[1]

Received: 27 October 2015 / Accepted: 30 November 2015 / Published online: 15 December 2015
© Springer International Publishing Switzerland 2015

Abstract Three new Co(II) coordination polymers, $[Co(L1)(bpdc)]_n$ (**1**), $[Co(L2)(ndc)(H_2O)\cdot 2H_2O]_n$ (**2**) and $[Co(L3)(ndc)(H_2O)\cdot H_2O]_n$ (**3**) (L1 = 1,2-bis(5,6-dimethylbenzimidazole)ethane, L2 = 1,3-bis(5,6-dimethylbenzimidazole)propane, L3 = 1,4-bis(5,6-dimethylbenzimidazole) butane, H_2bpdc = 4,4′-biphenyldicarboxylic acid, H_2ndc = 2,6-naphthalenedicarboxylic acid) have been synthesized under hydrothermal conditions and structurally characterized by X-ray crystallography. All three complexes feature (4,4) networks that extend into 3D supramolecular frameworks via hydrogen bonding interactions. The luminescence properties and catalytic activities of these complexes with respect to the degradation of methyl orange in a Fenton-like process have been investigated.

Introduction

The rational design and construction of coordination polymers (CPs) continue to attract much interest, due to the endless possibilities and nearly inexhaustible synthesis options for tailoring their structures and properties [1–4]. Much of the effort toward this goal was concentrated on crystal engineering, and there has been an increasing trend toward the synthesis of coordination polymers containing benzimidazole ligands [5–7]. In particular, the flexible bis(5,6-dimethylbenzimidazole) ligands with two N-donor sites have freely rotating methylene groups, so they can adopt various conformations to coordinate to different metal centers, which is beneficial for the construction of extended architectures [8–11]. A number of CPs with interesting structures and properties derived from these ligands have been prepared and characterized. However, the systematic synthesis of such compounds still presents a significant long-term challenge [12–15].

In general, it has been recognized that intermolecular forces such as hydrogen bonding interactions can be used as structure directing tools in the formation of coordination polymers of higher dimensionality [16–18]. The π–π stacking interaction is also an important and powerful non-covalent intermolecular interaction for the direction of supramolecular architectures [19–21]. A successful strategy for the construction of such coordination polymers is to employ appropriate functional ligands having strong coordination ability as well as hydrogen bond acceptors/donors and π-conjugated systems for extension of their networks. Multifunctional aromatic dicarboxylic acids with various coordinating modes and strong coordination capability are usually chosen as co-ligands with N-heterocyclic neutral ligands; the corresponding carboxylate conjugate bases are excellent hydrogen bond acceptors [22–25].

In this report, we introduce bis(5,6-dimethylbenzimidazole)-based ligands with different $-(CH_2)_n-$ (n = 2, 3, 4) spacers, with a view to an exploration of the influence of spacer length on the structures of their ternary mixed-ligand coordination polymers. Three new cobalt(II) coordination polymers have been hydrothermally synthesized and characterized, namely $[Co(L1)(bpdc)]_n$ (**1**), $[Co(L2)(ndc)(H_2O)\cdot 2H_2O]_n$ (**2**) and $[Co(L3)(ndc)(H_2O)\cdot H_2O]_n$ (**3**) (L1 = 1,2-bis(5,6-dimethylbenzimidazole)ethane, L2 = 1,3-bis(5,6-dimethylbenzimidazole)propane, L3 = 1,4-

✉ Guang Hua Cui
tscghua@126.com

[1] College of Chemical Engineering, North China University of Science and Technology, Tangshan 063009, Hebei, China

[2] Department of Inorganic and Physical Chemistry, Ghent University, Krijgslaan 281 S3, 9000 Ghent, Belgium

bis(5,6-dimethylbenzimidazole)butane, H_2bpdc = 4,4′-biphenyldicarboxylic acid, H_2ndc = 2,6-naphthalenedicarboxylic acid). The structures of these ligands are shown in Scheme 1. Considerations relevant to their stepwise assembly and structural correlations are discussed. The luminescence properties and catalytic activities of the complexes are also presented.

Experimental

Materials and methods

All the chemicals and reagents employed were purchased from Sinopharm Chemical Reagent Co., Ltd. and used as received without further purification. L1, L2 and L3 were synthesized according to the literature procedure [26]. Elemental analyses (C, H and N) were performed on a Perkin-Elmer 240C Elemental Analyzer. IR spectra (KBr pellets) were recorded on an Avatar 360 (Nicolet) spectrophotometer in the range of 4000–400 cm^{-1}. X-ray powder diffraction (XRPD) investigations were carried out on a Rigaku D/Max-2500PC X-ray diffractometer at 40 kV, 40 mA with Cu-Kα radiation (λ = 1.542 Å). Thermogravimetric analyses (TGA) were carried out on a NETZSCH TG 209 thermal analyzer in flowing N_2 with a heating rate of 10 °C/min. A Hitachi F-7000 fluorescence spectrophotometer was used for powdered solid samples at room temperature to obtain luminescence spectra. The absorptivity value of methyl orange was recorded with a Shanghai Jingke 722 N spectrophotometer at the maximum wavelength of 506 nm.

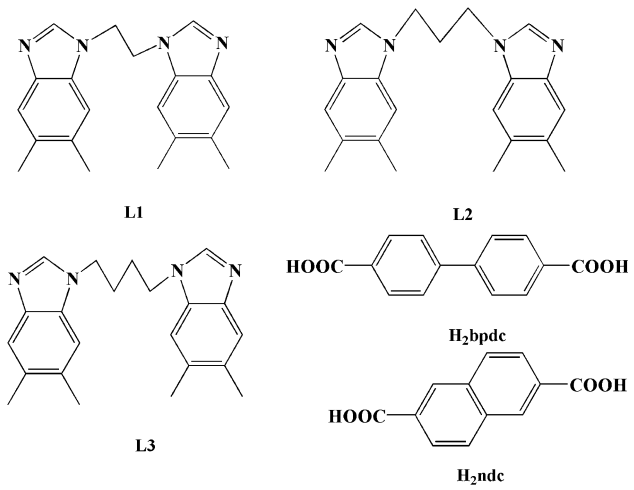

Scheme 1 The structural formulae of L1, L2, L3, H_2bpdc, H_2ndc

Synthesis of $[Co(L1)(bpdc)]_n$ (1)

A mixture of $Co(OAc)_2{\cdot}4H_2O$ (49.2 mg, 0.2 mmol), L1 (32.3 mg, 0.1 mmol), H_2bpdc (48.4 mg, 0.2 mmol), NaOH (8.0 mg, 0.2 mmol), ethanol (4 mL) and water (10 mL) was heated at 140 °C for 3 days in a 25 mL Teflon-lined vessel container. The mixture was then cooled to room temperature at a rate of 5 °C/h. Purple crystals suitable for single-crystal X-ray diffraction were obtained by filtration and washed with distilled water in 58 % yield (based on $Co(OAc)_2{\cdot}4H_2O$). Calcd. for $C_{34}H_{30}CoN_4O_4$ (Fw = 617.55): C 66.1, H 4.9, N 9.1 %. Found: C 65.9, H 5.1, N 9.3 %. IR (KBr, cm^{-1}): 1605 s, 1560 m, 1510 m, 1430 m, 1300 m, 1178 w, 847 w, 758 m.

Synthesis of $[Co(L2)(ndc)(H_2O){\cdot}2H_2O]_n$ (2)

A mixture of $CoSO_4{\cdot}7H_2O$ (56.7 mg, 0.2 mmol), L2 (33.8 mg, 0.1 mmol), 2,6-H_2ndc (43.7 mg, 0.2 mmol), NaOH (8.0 mg, 0.2 mmol) and water (10 mL) was heated at 140 °C for 3 days in a 25 mL Teflon-lined vessel container. The mixture was then cooled to room temperature at a rate of 5 °C/h. Purple block crystals of **2** were separated in 46 % yield based on $CoSO_4{\cdot}7H_2O$. Calcd. for $C_{33}H_{36}CoN_4O_7$ (Fw = 659.59): C 60.1, H 5.5, N 8.5 %. Found: C 59.9, H 5.2, N 8.7 %. IR (KBr, cm^{-1}): 3437 s, 1605 m, 1570 s, 1510 m, 1472 m, 1400 s, 1220 m, 1060 w, 1053 m, 997 w, 795 s, 621 w, 480 w.

Synthesis of $[Co(L3)(ndc)(H_2O){\cdot}H_2O]_n$ (3)

The synthesis of **3** was similar to that of **2**, but using L3 (0.1 mmol, 35.7 mg) in place of L2. Purple block crystals of **3** suitable for single-crystal X-ray diffraction were isolated in 54 % yield based on $CoSO_4{\cdot}7H_2O$. Calcd. for $C_{34}H_{36}CoN_4O_6$ (Fw = 655.60): C 62.3, H 5.5, N 8.6 %. Found: C 62.0, H 5.1, N 8.9 %. IR (KBr, cm^{-1}): 3389 s, 3110 w, 1605 m, 1560 s, 1520 m, 1470 m, 1390 s, 1353 s, 1273 m, 1229 m, 933 w, 791 s, 459 w.

X-ray crystallography

Crystallographic data for the complexes were collected on an Agilent SuperNova Dual diffractometer using mirror-monochromated Cu-Kα radiation (λ = 1.54178 Å) at room temperature with an Atlas detector in ω scan mode. All structures were solved by direct methods and refined on F^2 by full-matrix least-squares procedures with the SHELXTL program package [27]. Atoms were located from iterative examination of difference F-maps following least-squares refinements of the earlier models. Anisotropic parameters were used for non-hydrogen atoms, hydrogen atoms of water were located on a difference Fourier map, while

other H atoms were included in calculated positions and refined with fixed thermal parameters, each riding on a corresponding parent atom. The two lattice water molecules in complex **2** and one water molecule in complex **3** are disordered; these structures were refined by the SQUEEZE routine of PLATON [28]. The crystallographic data are listed in Table 1, and selected bond lengths and angles are presented in Table 2.

Catalysis experiments

The catalytic reactions were performed through a typical process as follows: 60 mg powder of the required complex and 2 mL of 30 % (w/w) H_2O_2 were mixed together with 200 mL of an aqueous solution of methyl orange (20 mg/L). The solution was kept continuously stirring with a magnetic stirrer, the temperature was constant at 40 °C and the pH was adjusted to 6.0. At given time intervals, 2 mL aliquots were removed and centrifuged to remove the residual catalyst, then measured for absorbance at 506 nm using a Shanghai Jingke 722 N visible spectrophotometer. A control experiment was also carried out under the standard conditions without any catalyst. The degradation efficiency of methyl orange was evaluated based on the following formula:

$$\text{Degradation efficiency} = \frac{(C_0 - C_t)}{C_0} \times 100\ \%$$

where C_0 (mg/L) is the initial concentration of methyl orange and C_t (mg/L) is the concentration of methyl orange at the reaction time, t (min).

Results and discussion

Synthesis of the polymers

The hydrothermal method has been extensively explored as a powerful tool in the self-assembly of CPs. By varying the molar ratio/composition of the initial reactants, reaction time and/or temperature, single crystals of complexes **1–3** suitable for single-crystal X-ray diffraction analysis were successfully obtained. It is noteworthy that NaOH solution was used in the preparation of these complexes, in order to deprotonate the carboxylic group, while the ethanol solvent in complex **1** may help to control the crystal shape.

Table 1 Crystal and refinement data for complexes **1–3**

Complex	**1**	**2**	**3**
Chemical formula	$C_{34}H_{30}CoN_4O_4$	$C_{33}H_{36}CoN_4O_7$	$C_{34}H_{36}CoN_4O_6$
Formula weight	617.55	659.59	655.60
Crystal system	Orthorhombic	Triclinic	Monoclinic
Space group	*Pcca*	$P\bar{1}$	P_{21}
a (Å)	28.4320(5)	5.6861(3)	5.9807(5)
b (Å)	7.8836(2)	11.4289(6)	19.4161(13)
c (Å)	12.2935(3)	13.0083(7)	13.1638(7)
α (°)	90	65.132(5)	90
β (°)	90	83.863(4)	93.821(6)
γ (°)	90	87.215(4)	90
V (Å^3)	2755.55(11)	762.57(7)	1525.21(18)
Z	4	1	2
D_{calcd} (g/cm^3)	1.489	1.436	1.428
Absorption coefficient (mm^{-1})	5.282	4.880	4.851
F(000)	1284	345	686
Crystal size (mm)	0.23 × 0.22 × 0.20	0.17 × 0.17 × 0.16	0.20 × 0.19 × 0.17
θ range (°)	3.11–67.07	3.76–67.07	3.36–75.65
Index range h, k, l	−33/33, −9/9, −11/14	−6/6, −13/13, −15/13	−7/7, −24/20, −16/16
Reflections collected	18,494	8244	11,964
Independent reflections (R_{int})	2474 (0.0588)	3933(0.0392)	5469(0.0505)
Data/restraint/parameters	2474/0/198	3933/6/398	5469/4/406
Goodness-of-fit on F^2	1.084	1.040	1.022
Final R_1, wR_2 ($I > 2\sigma(I)$)	0.0444, 0.1111	0.0520, 0.1225	0.0670, 0.1744
Largest diff. peak and hole	0.845, −0.440	1.399, −0.962	0.869, −0.629

Table 2 Selected bond lengths (Å) and angles (°) for complexes **1–3**

Parameter	Value	Parameter	Value
1			
Co(1)–N(1)A	2.091(2)	Co(1)–N(1)	2.091(2)
Co(1)–O(2)A	2.1535(2)	Co(1)–O(2)	2.1536(2)
Co(1)–O(1)	2.2177(2)	Co(1)–O(1)A	2.2177(2)
N(1)A–Co(1)–N(1)	105.96(11)	N(1)A–Co(1)–O(2)A	91.95(8)
N(1)–Co(1)–O(2)A	87.10(8)	N(1)A–Co(1)–O(2)	87.10(8)
N(1)–Co(1)–O(2)	91.95(8)	O(2)A–Co(1)–O(2)	178.43(11)
N(1)A–Co(1)–O(1)	141.30(8)	N(1)–Co(1)–O(1)	95.69(8)
O(2)–Co(1)–O(1)	60.01(7)	O(2)A–Co(1)–O(1)	121.32(8)
N(1)A–Co(1)–O(1)A	95.68(8)	N(1)–Co(1)–O(1)A	141.30(8)
O(2)A–Co(1)–O(1)A	60.01(7)	O(2)–Co(1)–O(1)A	121.33(8)
O(1)–Co(1)–O(1)A	86.16(10)		
2			
Co(1)–O(1W)	2.031(4)	Co(1)–O(2)A	2.050(4)
Co(1)–N(1)	2.108(5)	Co(1)–N(3)B	2.127(5)
Co(1)–O(4)	2.179(4)	Co(1)–O(3)	2.300(4)
O(1W)–Co(1)–O(2)A	90.54(18)	O(1W)–Co(1)–N(1)	97.83(18)
O(2)A–Co(1)–N(1)	86.15(18)	O(1W)–Co(1)–N(3)B	94.04(19)
O(2)A–Co(1)–N(3)B	87.85(18)	N(1)–Co(1)–N(3)B	166.74(19)
O(1W)–Co(1)–O(4)	88.94(16)	O(2)A–Co(1)–O(4)	176.08(19)
N(1)–Co(1)–O(4)	90.07(18)	N(3)B–Co(1)–O(4)	96.06(17)
O(1W)–Co(1)–O(3)	146.91(15)	O(2)A–Co(1)–O(3)	122.39(17)
N(1)–Co(1)–O(3)	88.39(17)	N(3)B–Co(1)–O(3)	84.86(17)
O(4)–Co(1)–O(3)	58.45(14)		
3			
Co(1)–O(4)A	2.069(4)	Co(1)–O(1W)	2.093(4)
Co(1)–N(4)B	2.104(6)	Co(1)–N(1)	2.121(6)
Co(1)–O(1)	2.137(3)	Co(1)–O(2)	2.268(3)
O(4)A–Co(1)–O(1W)	92.94(16)	O(4)A–Co(1)–N(4)B	87.2(2)
O(1W)–Co(1)–N(4)B	90.8(2)	O(4)A–Co(1)–N(1)	89.2(2)
O(1W)–Co(1)–N(1)	92.5(2)	N(4)B–Co(1)–N(1)	175.3(2)
O(4)A–Co(1)–O(1)	174.97(19)	O(1W)–Co(1)–O(1)	91.59(14)
N(4)B–Co(1)–O(1)	90.5(2)	N(1)–Co(1)–O(1)	92.8(2)
O(4)A–Co(1)–O(2)	115.27(16)	O(1W)–Co(1)–O(2)	151.61(14)
N(4)B–Co(1)–O(2)	93.47(19)	N(1)–Co(1)–O(2)	85.25(19)
O(1)–Co(1)–O(2)	60.35(13)		

Symmetry codes for **1**: A: $-x + 3/2, -y + 1, z$; for **2**: A: $x, y + 1, z - 1$; B: $x, y + 1, z$; for **3**: A: $x, y, z + 1$; B: $-x, y - 1/2, -z + 2$

Without it, only unformed powders were obtained under hydrothermal conditions. These compounds are stable in air and insoluble in water and general organic solvent, such as benzene, alcohol, dichloromethane and acetonitrile.

Crystal structure of complex 1

X-ray single-crystal structure analysis reveals that complex **1** crystallizes in the orthorhombic *Pcca* space group and its asymmetric unit contains half a [Co(L1)(bpdc)] molecule. As shown in Fig. 1a, the Co(II) center is six-coordinated by two nitrogen atoms (N1, N(1)A) from two separate L1 ligands and four oxygen atoms (O1, O2, O1A, O2A) from two anionic $bpdc^{2-}$ ligands to form a $\{CoN_2O_4\}$ trigonal prismatic geometry [29] (symmetry code: A: $-x + 3/2, -y + 1, z$). The Co–N bond length is 2.091(2) Å, and the Co–O bond lengths range from 2.1535(2) to 2.2177(2) Å. The bond angles around the Co1 center are well matched to those observed in similar complexes [30]. The ligand L1 employs *trans*-conformation such that the mean dihedral

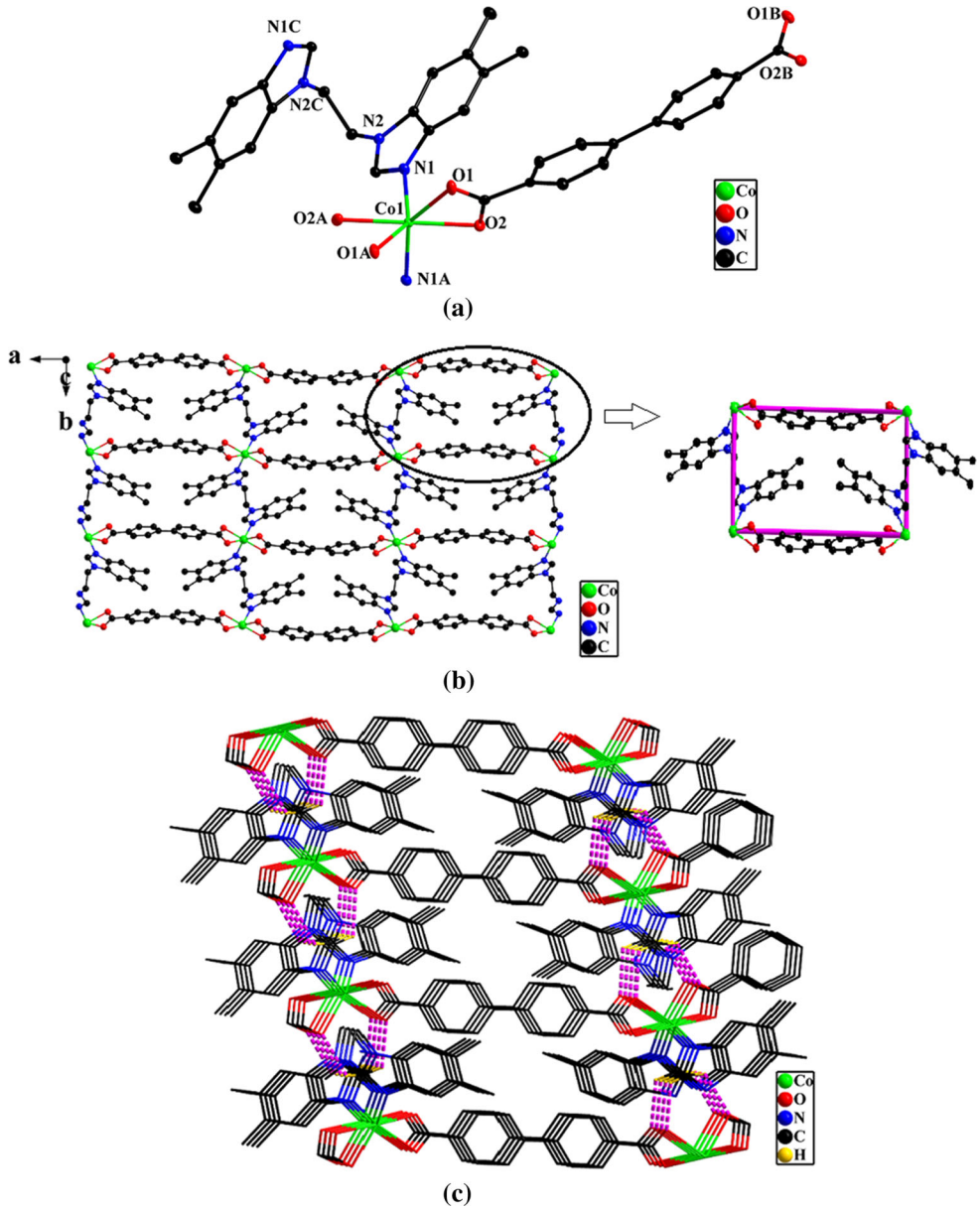

Fig. 1 **a** Coordination environment around the Co(II) centers in complex **1**. Hydrogen atoms are omitted for clarity (symmetry code: A: $-x + 3/2, -y + 1, z$; B: $-x + 1, y, -z + 1/2$; C: $-x + 3/2, -y, z$). **b** The 2D (4,4) layer structure of **1**. **c** View of the 3D supramolecular framework formed through C–H···O interactions. The *dashed lines* indicate C–H···O interactions

angle between the two benzimidazole rings is 59.06(5)°; by acting as a μ_2-bridging ligand, L1 bridges adjacent Co(II) centers to form a 1D infinite linear $[Co(L1)]_n$ chain. The benzimidazole rings of L1 are slightly twisted over each other by a torsion angle of 43.11(3)°. The $bpdc^{2-}$ ligands also connect neighboring Co(II) atoms to shape a 1D linear $[Co(bpdc)]_n$ chain, in which the $bpdc^{2-}$ ligands adopt the bis-chelating coordination mode. The two different types of 1D chain cross each other, resulting in a 2D grid structure. To better understand the structure of complex **1**, topological analysis was used [31]. All Co(II) centers can be simplified to 4-connected nodes and the shortest circuit is a four-membered ring, such that the 2D layer can be simplified to a 4^4-**sql** net with a mesh size of 7.8836 × 14.9962 Å (Fig. 1b). Weak intermolecular C–H···O hydrogen bonding interactions between the imidazole groups and carboxylate oxygen atoms of the $bpdc^{2-}$ ligands generate the overall 3D supramolecular framework of complex **1** [H8–O1B = 2.44 Å, C8–H8···O1B = 123°, symmetry code: B: $-x + 2/3, y, z - 1/2$].

Crystal structure of complex 2

Complex **2** crystallizes in the triclinic $P\bar{1}$ space group, and the asymmetric unit is composed of a cobalt atom, one neutral L2 ligand, one ndc^{2-} ligand, one coordinated water ligand and two lattice water molecules. As depicted in Fig. 2a, the Co(II) center is six-coordinated by three O atoms (O2A, O3, O4) from two anionic ndc^{2-} ligands, one O1W from a water ligand and two N atoms (N1, N3B) from two different L2 ligands (symmetry codes: A: x, $y + 1$, $z - 1$; B: x, $y + 1$, z). A distorted $\{CoO_4N_2\}$ octahedral coordination environment is observed at the cobalt atom, with two nitrogen atoms in the axial positions and four oxygen atoms in the equatorial plane. The Co–N bond lengths are 2.108(5) and 2.127(5) Å, and the Co–O distances fall in the range of 2.031(4)–2.300(4) Å. For the ndc^{2-} ligand, the coordination modes of the two carboxyl groups are different: one coordinates to a Co(II) center in a monodentate mode, while the other coordinates to a different Co(II) center in a chelating fashion. The ndc^{2-} ligands bridge neighboring Co(II) atoms to give a $[Co(ndc^{2-})]_n$ straight chain in which the Co···Co distance is 13.2210 Å. In addition, L2 acts as a bidentate μ_2-*N*,*N′* bridging ligand to link the adjacent two Co(II) centers into a $[Co(L2)]_n$ zigzag chain, and the dihedral angle between two benzimidazole rings is 82.71(9)°. The contiguous $[Co(L2)]_n$ chains are bridged by ndc^{2-} ligands forming a (4,4) grid structure (Fig. 2b). These neighboring layers are extended into a 3D supramolecular network (Fig. 2c) through hydrogen bonds between the carboxyl oxygen atoms (O1, O3) from ndc^{2-} ligands and the O1W from the water ligand [O1W–H1WA···O1C = 2.636(7) Å, O1W–H1WB···O3D = 2.636(7) Å, symmetry codes: C: $x - 1$, $y + 1$, $z - 1$; D: $x - 1$, y, z].

Crystal structure of complex 3

Single-crystal X-ray diffraction analysis shows that complex **3** crystallizes in the monoclinic P_{21} space group. The asymmetric unit contains one Co(II) atom, a complete L3 ligand, one ndc^{2-} ligand, one water ligand and one lattice water. Similar to **2**, complex **3** possesses a distorted octahedral {CoO4N2} coordination geometry (Fig. 3a), in which each Co(II) atom is coordinated by four oxygen atoms from two different ndc^{2-} ligands in the equatorial plane [Co(1)–O(4)A = 2.069(4) Å, Co(1)–O(1W) = 2.093(4) Å, Co(1)–O(1) = 2.137(3) Å, Co(1)–O(2) = 2.268(3) Å] and two nitrogen atoms from L3 ligands in the axial position [Co(1)–N(4)B = 2.104(6) Å, Co(1)–N(1) = 2.121(6) Å] (symmetry codes: A: x, y, $z + 1$; B: $-x$, $y - 1/2$, $-z + 2$).

The N-donor ligands connect cobalt(II) atoms in a bis(monodentate) binding mode to form a 1D Ω-like chain along the *b*-axis such that the dihedral angle between the benzimidazole rings of the L3 ligand is 7.06(2)°. Each ndc^{2-} moiety serves as a chelating-monodentate ligand to join two Co(II) atoms, such that the ndc^{2-} ligands span a Co···Co internuclear distance of 13.1638 Å and form a

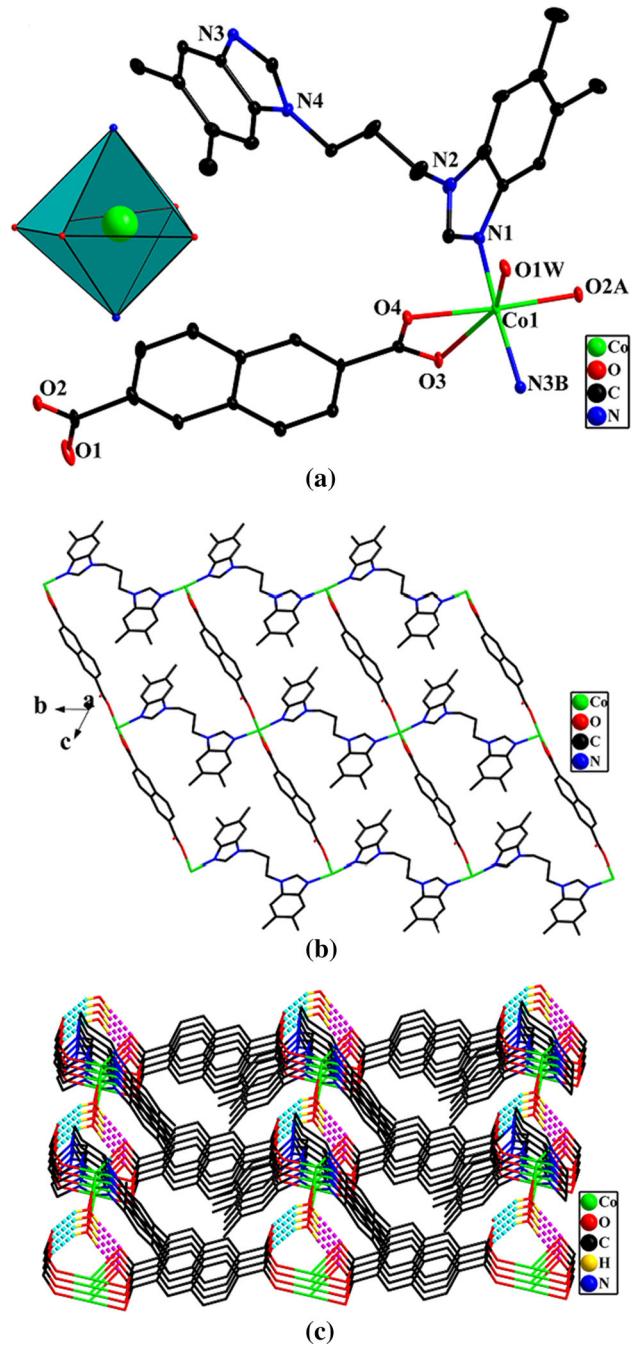

Fig. 2 **a** Coordination environment around the Co(II) centers in complex **2**. Hydrogen atoms are omitted for clarity (symmetry code: A: x, $y + 1$, $z - 1$; B: x, $y + 1$, z). **b** A schematic drawing of the 2D layer-like structure in **2**. **c** The 3D supramolecular network of **2**, constructed by C–H···O hydrogen bonding interactions. The *dashed lines* indicate C–H···O bonds

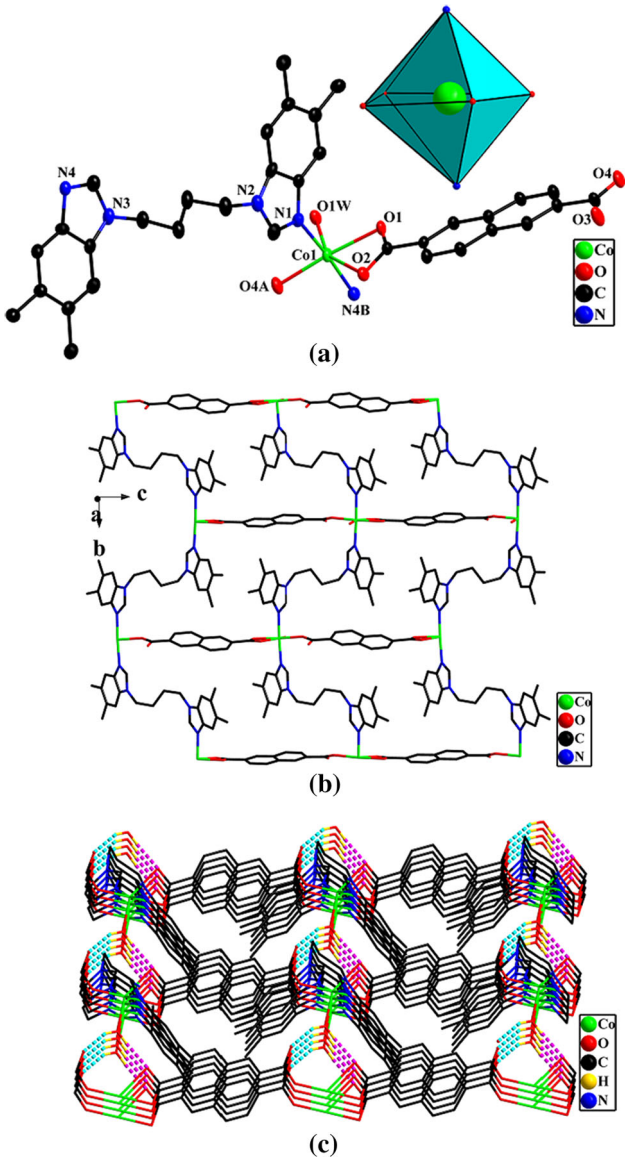

Fig. 3 **a** Coordination environment around the Co(II) centers in complex **3**. Hydrogen atoms are omitted for clarity (symmetry code: A: $x, y, z + 1$; B: $-x, y - 1/2, -z + 2$). **b** View of the 2D layer-like structure in **3**. **c** The 3D supramolecular network of **3**, constructed by C–H···O hydrogen bonding interactions. The *dashed lines* indicate C–H···O bonds

neutral $[Co(ndc^{2-})]_n$ coordination polymer chain arranged along the *c* direction. These two chains propagate into a 2D 4^4 grid-like layer, arranged in an offset way with the grid occupied by groups from the adjacent chains (Fig. 3b). Complex **3** displays a uninodal 2D layer with a (4,4) topology, and the rectangular window of the 2D motif has dimensions of ca. 11.7235 × 13.1638 Å. Aggregation between layers is promoted by classical hydrogen bonding interactions provided by the oxygen atom of the lattice water molecule, which serves as a hydrogen bonding donor to the oxygen atom from ndc^{2-} [O1W–H1WA···O3C = 2.672(6) Å, O1W–H1WB···O2D = 2.771(5) Å, symmetry codes: C: $x - 1, y, z + 1$; D: $x - 1, y, z$]. In this manner, the 2D network is further extended into a 3D supramolecular architecture.

To summarize, three flexible bis(benzimidazole) ligands (L1, L2, and L3) with different $-(CH_2)_n-$ spacers ($n = 2, 3, 4$) gave three cobalt(II) complexes. All three complexes have 2D layered structures and exhibit typical 4^4 **sql** topology. In complex **1**, the $bpdc^{2-}$ ligand adopts the bis-chelating coordination mode, while the ndc^{2-} ligand employs the same chelating-monodentate coordination mode for complexes **2** and **3**. For all three complexes, all the bis(benzimidazole) ligands adopt the bidentate bridging mode, connecting the Co(II) centers with Co···Co distances of 7.8836(2) Å for **1**, 11.4289(15) Å for **2**, 11.7235(16) Å for **3** (Table 3). All the three complexes are self-assembled into 3D networks through C–H···O (for **1**) and O–H···O (for **2** and **3**) hydrogen bonding interactions.

IR spectra and X-ray powder diffraction studies

The IR spectra exhibit the main characteristic bands of water molecules, the carboxylate ligands and nitrogen-containing organic ligands expected for the title complexes. The bands at 3437 and 3389 cm^{-1} for complexes **2** and **3**, respectively, are attributed to the lattice water. There is no absorption band around 1700 cm^{-1} for any of these complexes, indicating that all carboxyl groups are completely deprotonated [32]. Strong peaks at 1605 and 1560 cm^{-1} for **1**, 1605, 1570, 1474 and 1400 cm^{-1} for **2**, 1605, 1560, 1470 and 1390 cm^{-1} for **3**, may be attributed to the asymmetric and symmetric vibrations of carboxylato groups. The separations ($\Delta\nu[\nu_{as}(COO)–\nu_s(COO)]$) between these bands indicate the presence of chelating (45 cm^{-1} for **1**) and chelate/monodentate (205 and 96 cm^{-1} for **2**; 215 and 90 cm^{-1} for **3**) carboxyl groups. The bands at ca. 1500 cm^{-1} for all three complexes are assigned to the $\nu_{(C=N)}$ stretches of the benzimidazole rings.

To determine whether the crystal structures are truly representative of the bulk materials used for property studies, X-ray powder diffraction (XRPD) experiments were carried out for the complexes. The XRPD experimental and as-simulated patterns are shown in Fig. 4. The crystalline samples of complexes **1–3** gave a positive match between the experimental and simulated XRPD patterns, indicating that the bulk synthesized material and the crystals are homogeneous.

Thermal and luminescence properties

To characterize the stabilities of complexes **1–3**, their thermal behaviors were investigated under nitrogen

Table 3 Coordination modes of dicarboxylic acids and bis(benzimidazole) ligands of complexes **1**–**3**

Complexes	Polycarboxylates	Bis(benzimidazole) ligands
1	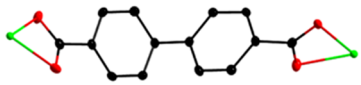	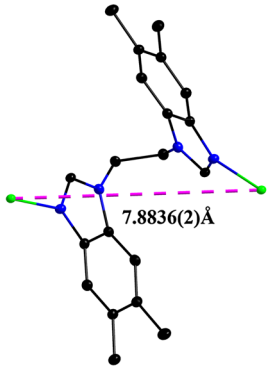
2	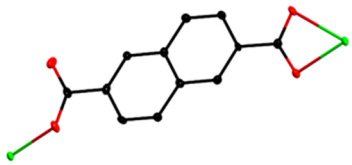	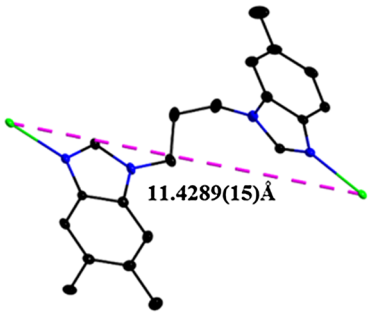
3	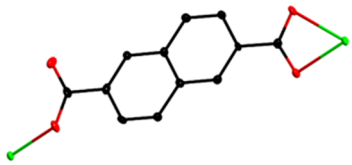	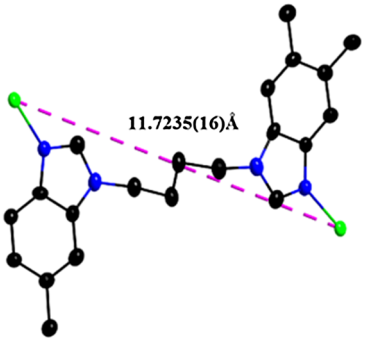

atmosphere by TGA. As depicted in Fig. 5, complex **1** remains stable up to 405 °C, finally decomposing to CoO as a residue (obsd 12.3 %, calcd 12.1 %). The TG curve for complex **2** shows a gradual weight loss between 95 and 160 °C, which can be ascribed to the loss of three water molecules (obsd 8.3 %, calcd 8.2 %). The loss of organic ligands occurs within the range of ca. 336–604 °C. The remaining weight corresponds to the formation of CoO (obsd 11.2 %, calcd 11.4 %). For complex **3**, the loss of two water molecules is observed within the range of 80–170 °C (obsd 5.6 %; calcd 5.5 %) and the decomposition of the compound occurs at 365 °C to give CoO residue (obsd 11.4 %; calcd 11.3 %).

The solid-state luminescence properties of both the complexes and free ligands have been investigated at room temperature. As shown in Fig. 6, free L1, L2, and L3 display luminescence with emission maxima at 389, 369, and 365 nm, respectively ($\lambda_{ex} = 315$ nm for L2 and L3, $\lambda_{ex} = 230$ nm for L1), attributed to $\pi^* \rightarrow \pi$ transitions [33, 34]. Recent studies have shown that solid H_2bpdc exhibits weak emission at 404 nm ($\lambda_{ex} = 335$ nm) [35]. Comparing with L1, the blue-shift of ca. 48 nm for complex **1** may be assigned to metal-to-ligand charge-transfer (MLCT). Red-shifts of ca. 33 nm for complex **2** and 35 nm for **3** are observed compared with L2 and L3, respectively, which can probably be assigned to intra-ligand ($\pi^* \rightarrow n$) luminescence emissions [36].

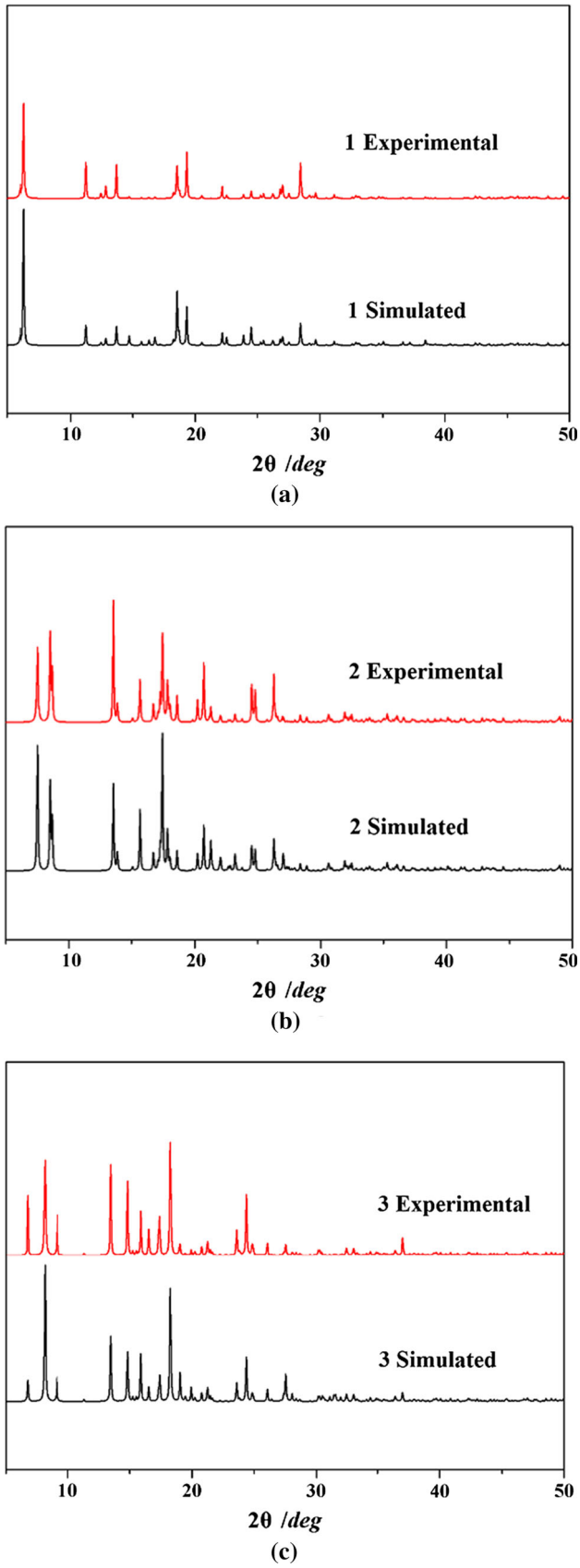

◀**Fig. 4** The powder X-ray diffraction patterns calculated from the single-crystal data and that obtained from the experiments for polymer **1**-**3**, respectively

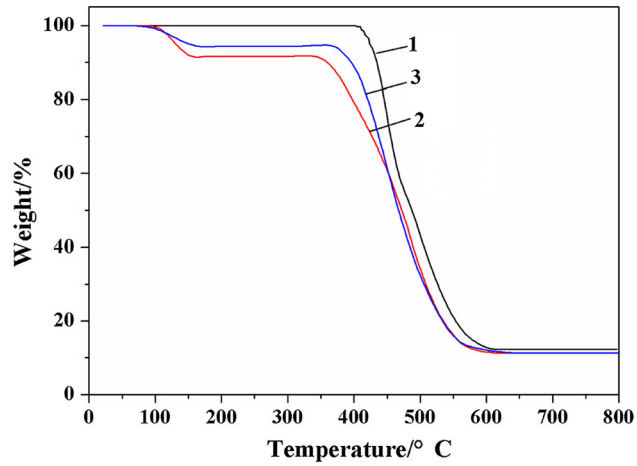

Fig. 5 The TGA curves of polymers **1**–**3**

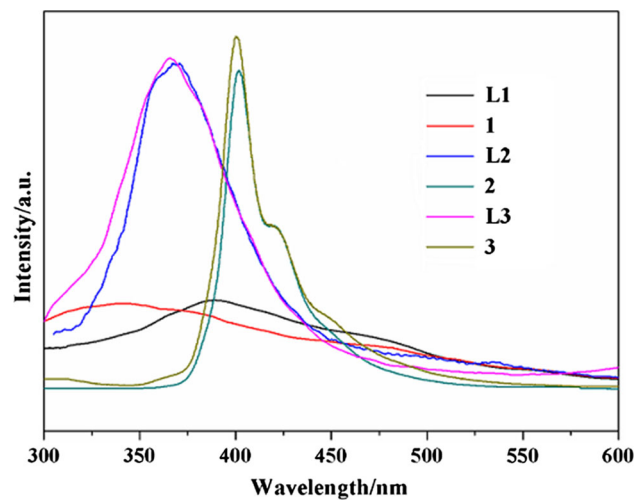

Fig. 6 Emission spectra of complexes **1**–**3** and the free ligands

Catalytic degradation properties

In recent years, much work has been carried out on advanced oxidation processes (AOPs) for the treatment of azo dye wastewaters. The Fenton-like reaction appears to be the most promising such AOP in terms of both cost-effectiveness and ease of operation. It involves the production of strongly oxidizing agents, mainly ·OH radicals, which react rapidly and non-selectively with most inorganic and organic compounds. The ·OH radical is

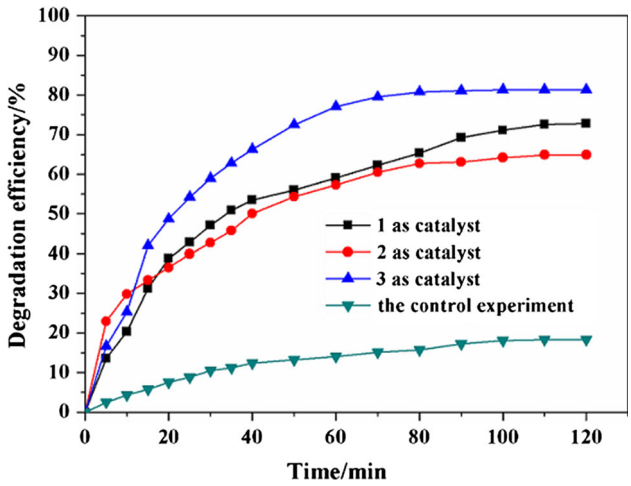

Fig. 7 Experimental results of the catalytic degradation of methyl red dye

sufficiently active as to destroy organic compounds into CO_2, H_2O and other products [37, 38]. In this work, we have chosen methyl orange (MO), as a model dye contaminant, in order to evaluate their catalytic effectiveness for AOP. The degradation efficiencies of MO against reaction time (*t*) for the title complexes are shown in Fig. 7. In the absence of any catalyst, there is no noticeable change in the absorbance of dye, and the self-degradation efficiency of control experiments in the presence of H_2O_2 only reaches 18.3 % after 120 min. When each of the complexes is added, a reaction takes place leading to loss of the dye color. Thus, approximately 81.3 % of MO has decomposed after 120 min for complex **3** as catalyst, 72.8 % for complex **1**, and 64.9 % for complex **2**. The catalytic activity of complex **3** is thus higher than complexes **1**, **2** and many other CPs that have been investigated [39, 40]. The differences in catalytic activities may be attributed to the different dicarboxylic acids and the various spacer lengths in the N-containing ligands, as well as the overall structures of these polymeric cobalt(II) complexes.

Conclusions

In conclusion, by introducing H_2bpdc and H_2ndc as mixed ligands, three Co(II) 2D coordination polymers based on flexible bis(5,6-dimethylbenzimidazole) ligands have been successfully synthesized. All three complexes present similar 2D grid structures, which are extended into 3D supramolecular frameworks through hydrogen bonding interactions. Complex **3** shows higher catalytic activity than **1**, **2** and many other CPs in the Fenton-like process for decomposition of dye [41].

Supplementary materials

CCDC 1427142-1427144 contain the supplementary crystallographic data for the complexes **1**-**3**. These data can be obtained free of charge via http://www.ccdc.cam.ac.uk/conts/retrieving.html, or from the Cambridge Crystallographic Data Centre, 12 Union Road, Cambridge CB2 1EZ, UK; fax: (+44) 1223-336-033; or e-mail: deposit@ccdc.cam.ac.uk.

Acknowledgments The project was supported by the National Natural Science Foundation of China (51474086), Natural Science Foundation-Steel and Iron Foundation of Hebei Province (B2015209299), the Graduate Student Innovation Fund of North China University of Science and Technology (2015S13) and the Hercules Foundation (project AUGE/11/029 "3D-SPACE: 3D Structural Platform Aiming for Chemical Excellence") and the Research Fund-Flanders (FWO) for funding.

References

1. Zhu QL, Xu Q (2014) Chem Soc Rev 43:5468–5512
2. Zhang T, Lin W (2014) Chem Soc Rev 43:5982–5993
3. Li M, Li D, O'Keeffe M, Yaghi OM (2014) Chem Rev 114:1343–1370
4. Lin HY, Luan J, Wang XL, Zhang JW, Liu GC, Tian AX (2014) RSC Adv 4:62430–62445
5. Yang FF, Yu XY, Luo YH, Wang XF, Sun DH, Zhang H (2015) Polyhedron 85:337–346
6. Zhang JW, Gong CH, Hou LL, Tian AX, Wang XL (2013) J Solid State Chem 205:104–109
7. Yang YQ, Yang J, Kan WQ, Yang Y, Guo J, Ma JF (2013) Eur J Inorg Chem 2013:280–292
8. Li M, Zhao S, Peng YF, Li BL, Li HY (2013) Dalton Trans 42:9771–9776
9. Li M, Ling Q, Yang Z, Li BL, Li HY (2013) CrystEngComm 15:3630–3639
10. Nobakht V, Beheshti A, Proserpio DM, Carlucci L, Abrahams CT (2014) Inorg Chim Acta 414:217–225
11. Meng W, Xu Z, Ding J, Wu D, Han X, Hou H, Fan Y (2014) Cryst Growth Des 14:730–738
12. Wang XX, Yu BY, Hecke KV, Cui GH (2014) RSC Adv 4:61281–61289
13. Hao JM, Yu BY, Hecke KV, Cui GH (2015) CrystEngComm 17:2279–2293
14. Qin L, Liu LW, Du X, Cui GH (2012) Transit Met Chem 38:85–91
15. Xiao SL, Li YH, Ma PJ, Cui GH (2013) Inorg Chem Commun 37:54–58
16. Wang XX, Liu YG, Ge M, Cui GH (2015) Chin J Inorg Chem 31:2065–2072
17. Atwood JL, Barbour LJ, Jerga A (2004) Angew Chem Int Ed 116:3008–3010
18. Sherrington DC, Taskinen KA (2001) Chem Soc Rev 30:83–93
19. Yang J, Ma JF, Liu YY, Ma JC, Batten SR (2007) Inorg Chem 46:6542–6555
20. Liu LL, Huang JJ, Wang XL, Liu GC, Yang S, Lin HY (2013) Inorg Chim Acta 394:715–722
21. Shi WJ, Hou L, Li D, Yin YG (2007) Inorg Chim Acta 360:588–598
22. Han J, Yau CW, Chan CW, Mak TCW (2012) Cryst Growth Des 12:4457–4465

23. Okuno T, Sakoda Y, Kinuta T, Sato T, Tokutome H, Tajima N, Nakano Y, Fujiki M, Kuroda R, Imai Y (2012) CrystEngComm 14:4819–4825
24. Wang XX, Yu YM, Huan DH, Hecke KV, Cui GH (2015) Inorg Chem Commun 61:24–26
25. Shiota N, Okuno T, Kinuta T, Sato T, Kuroda R, Matsubara Y, Imai Y (2011) CrystEngComm 13:1683–1686
26. Aakeroy CB, Desper J, Elisabeth E, Helfrich BA, Levin B, Urbina JF (2005) Z Kristallogr 220:325–374
27. Sheldrick GM (2008) Acta Cryst A 64:112–122
28. Spek AL (2000) PLATON. Utrecht University, Utrecht
29. Banerjee S, Ghosh A, Wu B, Lassahn PG, Janiak C (2005) Polyhedron 24:593–599
30. Wang XL, Sui FF, Lin HY, Zhang JW, Liu GC (2014) Cryst Growth Des 14:3438–3452
31. Blatov VA (2012) Struct Chem 23(4):955–963
32. Liu GC, Huang JJ, Zhang JW, Wang XL, Lin HY (2013) Transit Met Chem 38:359–365
33. Liu HY, Wu H, Ma JF, Liu YY, Liu B, Yang J (2010) Cryst Growth Des 10:4795–4805
34. Allendorf MD, Bauer CA, Bhakta RK, Houk RJT (2009) Chem Soc Rev 38:1330–1352
35. Dai JC, Wu XT, Cui CP, Hu SM, Du WX, Wu LM, Zhang HH, Sun RQ (2002) Inorg Chem 41:1391–1396
36. Ugale B, Singh D, Nagaraja CM (2015) J Solid State Chem 226:273–278
37. Wu XY, Qi HX, Ning JJ, Wang JF, Ren ZG, Lang JP (2015) Appl Catal B 168:98–104
38. Qi HX, Wang JF, Ren ZG, Ning JJ, Lang JP (2015) Dalton Trans 44:5662–5671
39. Zhang X, Meng XL, Huang CM, Cui GH (2015) J Mol Struct 1100:94–99
40. Hao JM, Li YH, Li HH, Cui GH (2013) Transit Metal Chem 39:1–8
41. Wang CC, Li JR, ZhangYQ LuXL, Guo GS (2014) Energy Environ Sci 7:2831